# Contact Angle Dependence of the Resonant Frequency of Sessile Water Droplets

James S. Sharp,* David J. Farmer, and James Kelly

School of Physics and Astronomy and Nottingham Nanotechnology and Nanoscience Centre, University of Nottingham, University Park, Nottingham, NG7 2RD, United Kingdom

Ⓢ *Supporting Information*

ABSTRACT: The resonant vibrations of small (microliter) sessile water droplets supported on solid substrates were monitored using a simple optical detection technique. A small puff of air was used to apply an impulse to the droplets and their time dependent oscillations were monitored by passing a laser beam through the droplet and measuring the variations of the intensity of the scattered light using a simple photodiode arrangement. The resulting time dependent intensity changes were then Fourier transformed to obtain information about the vibrational frequencies of the droplets. The resonant frequencies of droplets with masses in the range $0.005-0.03$ g were obtained on surfaces with water contact angles ranging from $12 \pm 4°$ to $160 \pm 5°$. The contact angle dependence of the resonant frequency of the droplets was found to be in good agreement with a simple theory which considers standing wave states along the meridian profile length of the droplets.
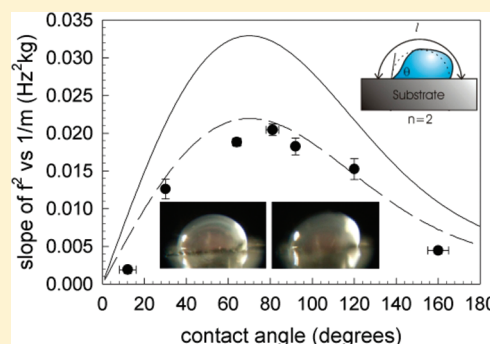
INTRODUCTION

Resonant vibrations of liquid droplets have received a significant amount of recent scientific interest. Studies of the behavior of isolated liquid droplets date back to the times of Lord Rayleigh.[1] However, much of the experimental and theoretical work that was performed on the resonant vibrations of droplets appears to have initially been motivated by studies of the effects of vibration on the formation of high purity crystals under zero gravity conditions.[2−4] A number of other potential applications of vibrating droplets have also been identified, including the possibility of using isolated droplets for electric field enhanced liquid−liquid extraction,[2] electrospray synthesis of mixed oxide ceramics, and for the measurement of surface tension[2,5] and contact angles.[6] This has led to a host of extremely elegant experiments involving the study of, for example, acoustically and magnetically levitated droplets.[5] More recently, a renewed interest in this field has been generated by studies of the actuation of small droplets on gradient energy surfaces.[7−9] The idea being that these surfaces have a gradient in wettability that is caused by either a chemical gradient or a gradient in topographical surface structure. When droplets are placed on these surfaces they display a contact angle which is dependent upon their position on the surface. Vibration of the droplets close to their resonant frequencies enables them to sample nearby conformations and has been shown to overcome pinning and contact angle hysteresis effects and to facilitate the motion of the droplet down the surface energy gradient.[8] As a result of this renewed interest, a number of authors have studied the resonant behavior of small liquid droplets on vibrated surfaces[2,6,10−12] and in electrically driven sessile droplets.[13,14] However, a serious limitation of these

studies has been that they are performed over a limited range of contact angles. In many cases, the experiments are restricted to studies of droplets vibrating on a single surface and hence, only one possible contact angle value.

The theory of droplet vibrations is well developed and the earliest theoretical interpretation of the resonant behavior of liquid droplets was provided by Lord Rayleigh and developed further by Chandrasekhar.[1] More recent studies by Strani and Sabetta[3] and Smithwick and co-workers[4] considered the vibration of sessile droplets in a spherical bowl. Although this theory was successfully extended to planar surfaces, determination of the contact angle dependent eigenvalues associated with the different vibrational modes of the droplet involved solving the determinant of an infinitely large matrix. A more recently developed model proposed by Noblin et al. offers a more intuitive interpretation of the origin of the vibrational modes of sessile droplets.[12] This theory considers the number of half integer wavelengths that can fit around the meridian profile length of a droplet and uses the dispersion relation for capillary waves in an infinitely deep liquid bath to obtain an approximation for the frequencies of the resonant vibrational modes.

Experimental work on sessile droplets has also been performed by a number of authors. For example, a range of studies have been performed on droplets that were either horizontally[7,10,15] or vertically[12,16] vibrated using a loudspeaker or surface acoustic wave generator.[6] Another method of driving the oscillations in

droplets involves the use of ac electric fields.[13,17] This method not only allows for the measurement of the resonant properties of small conducting liquid or "leaky" dielectric drops, but also facilitates control of their wetting interactions by changing the interfacial energies of the drops via the introduction of surface charges to the system. Methods of detection of the resonant modes have involved high speed image acquisition of the vibrating droplets,[7,12,15] optical deflection based techniques where a laser beam is passed through the droplet and its motion monitored using a position sensitive detector[6,16] and optical tweezer based approaches.[14] The studies on sessile droplets have been motivated by the need to develop a fundamental understanding of their resonant behavior and by a number of more practical applications. These include studies that were designed to use vibration to overcome contact angle hysteresis effects and enable the determination of equilibrium contact angle values,[6,12,17] actuation of the motion of liquid droplets on gradient surfaces[7,15] and to drive the internal mixing of multicomponent systems.[18] A recent study by Mchale and co-workers[13] has also studied vibrations in electrically driven "liquid marbles" with contact angles close to 180° in an attempt to use them as analogues of free/levitated drops.

This work describes an experimental study of the contact angle dependence of the resonant frequencies of sessile water droplets. A simple optical detection method is used to monitor the oscillations when a small impulse is applied to the droplets. This method is so simple that it can be easily implemented in any laboratory equipped with a laser, a photodiode and a data acquisition card—making the subject of these experiments suitable for use in undergraduate based projects. The novelty in this work lies in the measurement of the resonant vibrations of sessile droplets over a broad range of contact angles (~12−160°) and in the application of a modified version of the theory proposed by Noblin and co-workers[12] to the data. To the best of our knowledge, a detailed study over a broad range of contact angles has not been performed. We show that the functional dependence of the resonant frequency of sessile water droplets on contact angle is the same as that predicted by the simple theory and that the measured values of the lowest frequency modes agree with the predictions of the theory to within a constant numerical factor.

■ EXPERIMENTAL SECTION

Small microliter water droplets with masses in the range 0.005−0.03 g were placed on solid substrates and mounted on the surface of an analytical balance. In each case the mass of the droplet was recorded to within ±0.0001g, a laser beam (HeNe, 633 nm) was passed through the droplet, allowed to reflect off the substrate and the scattered light was collected using a low cost Silicon photodiode (RS Components, UK) attached to an amplifier and connected to a PC via a National Instruments USB-6008 data acquisition card (see Figure 1). The droplets were forced to vibrate by applying an impulse in the form of a small puff of air (by simply blowing on the droplet) and the time dependent oscillations of the intensity of light measured by the photodiode were recorded. Data were sampled over periods of 3−5 s using a sampling rate of 1kHz. The time dependent signal was then Fourier transformed to obtain information about the frequency dependence of the droplet oscillations. Each droplet was vibrated at least 3 times to ensure that the shapes and positions of the peaks in the spectra produced were reproducible. The droplets were then reweighed after each measurement to ensure that significant evaporation losses had not occurred during the experiments. Figure 1 shows an example of the time dependent signal obtained for a sessile water droplet supported on a
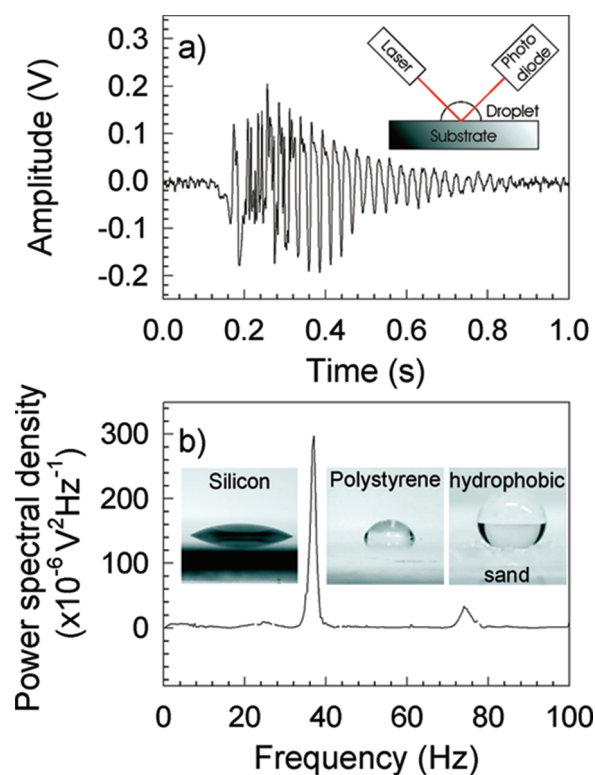

Figure 1. Oscillations of sessile water droplets. The inset in the panel (a) shows a schematic diagram of the experimental setup used to measure the oscillations of the droplets. Panel (a) also shows the time dependent signal measured by the photodiode for a $0.0140 \pm 0.0001g$ water droplet supported on a polystyrene substrate ($\theta = 81 \pm 3°$). A puff of air was applied to the droplet at a time $t \approx 0.1$ s. Panel (b) shows the frequency response of this droplet obtained by Fourier transformation of the data in panel (a). The dominant peak in this spectrum corresponds to the $n = 2$ vibrational mode of the droplet (see text). The insets in the panel show examples of images of droplets supported on Silicon, Polystyrene, and hydrophobic sand substrates. These images are similar to the ones that were used to determine the contact angle of the droplets on these surfaces.

polystyrene substrate (Figure 1a) along with its corresponding power spectrum (Figure 1b).

The above process was repeated for droplets of different mass that were supported on different solid substrates. The substrates that were used included spin-cast polymer films (all obtained from Polymer Source, Quebec), glass microscope slides, single crystal silicon wafers (Si, Compart Technology, UK,[100] orientation, native oxide intact), cured polydimethylsiloxane (PDMS, Sylgard 182, Dow Corning) surfaces, and a fine grade of hydrophobic sand. The spin-cast polymer films were prepared by dissolving Polystyrene (PS, 600 kDa) and Polymethylmethacrylate (PMMA, 600 kDa) in toluene and spin coating the resulting solutions on to a clean glass slide before annealing under vacuum at 120°C for 2 h. Glass microscope slides and Si wafers were used as supplied and PDMS films were prepared by mixing the resin and cross-linker in a 10:1 ratio before spreading onto a glass slide and annealing at 120 °C for 2 h. The hydrophobic sand is sold as a child's toy and is available under the trade name "Aqua Sand". This material is essentially a fine grade of sand which has been exposed to the vapors of Trimethylsilanol $(CH_3)_3SiOH$. A thin layer of PDMS was cast on to a clean glass slide and then coated with a thick layer of the hydrophobic sand. These layers were then compressed using a second glass slide and then the PDMS was left to cure overnight at room temperature. Once cured, any excess sand was gently removed leaving behind a glass slide that was completely coated with a thin layer of the hydrophobic sand.

Table 1. Measured Water Contact Angle Values for the Substrates Used in the Droplet Vibration Experiments

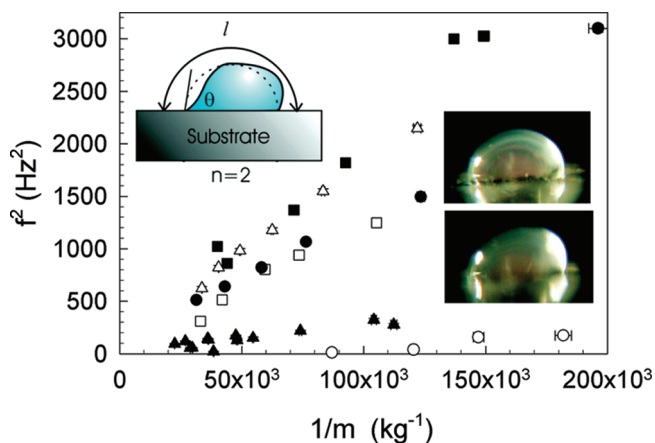| substrate	contact angle (deg)
glass	12 ± 4
silicon	30 ± 1
polymethylmethacrylate (PMMA)	64 ± 2
unannealed polystyrene (uPS)	81 ± 3
polystyrene (PS)	92 ± 1
polydimethylsiloxane (PDMS)	120 ± 1
hydrophobic sand	160 ± 5

Figure 2. Mass dependence of the resonant frequency of sessile droplets. Plots are shown for the square of the fundamental frequency (f) of the droplets vs the reciprocal of the droplet mass (m). Data are shown for droplets supported on glass ($\bigcirc$), Silicon ($\square$), PMMA ($\triangle$), PS ($\blacksquare$), PDMS ($\bullet$), and hydrophobic sand ($\blacktriangle$) substrates. The contact angles of water droplets on each of these surfaces are listed in Table 1. The inset in the top left of this figure shows the $n = 2$ vibrational mode of a droplet having a profile length, l and contact angle, θ. The images on the right are photographs of a 0.0122 g water droplet at rest (top image) and on a vertically vibrating PDMS surface (bottom image, frequency of vibration = 32.6 Hz).

The contact angle of water droplets was measured on each of the substrates by collecting an image of the droplet using a Philips SPC 1030NC webcam and then analyzing each image using Image Pro Plus 4.0 (Media Cybernetics). In each case, a small droplet was placed on the surface of the substrate and gently vibrated, prior to imaging, by applying short puffs of air similar to those used to vibrate the droplets above. Vibrating the droplets has been shown to overcome any contact line pinning effects and to give a uniform contact angle at all points along the three phase contact line.[12,19] In each case, the droplets were rotated to ensure that the contact angle was the same at both sides of the droplet and that it was the same within error when viewed from different directions. Each droplet was also vibrated again after measurement to ensure that the contact angle did not change. Table 1 gives details of the measured contact angles obtained on each surface along with their experimental uncertainties. Examples of images obtained from sessile droplets supported on silicon, polystyrene and hydrophobic sand substrates are shown as insets in Figure 1.

Changes in the droplet shapes were also studied by imaging a 0.0122 g water droplet on a PDMS surface which was mounted on a loudspeaker and vibrated vertically at a frequency of 32.6 Hz. The driving signal was provided by a signal generator and home-built power amplifier that were connected to the loudspeaker. Images were collected at a rate of 60
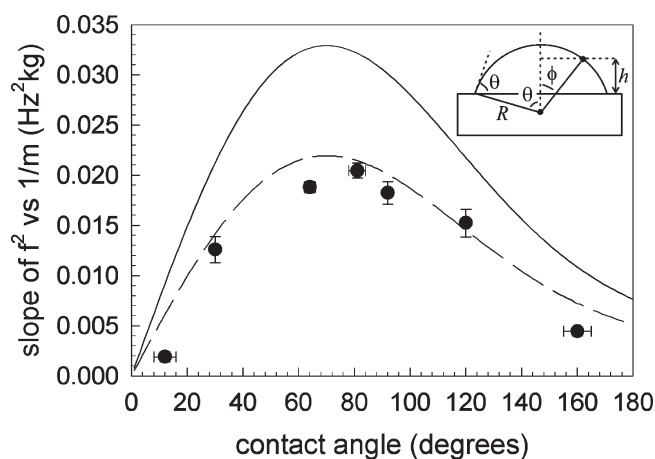

Figure 3. Contact angle dependence of the resonant frequency of sessile water droplets. The solid symbols are experimental data obtained from the slopes of the f^2 vs $1/m$ plots in Figure 2. The solid line represents the prediction of the simple theory obtained from eq 4 and the dashed line is the result of multiplying the solid line by a factor of $2/3$ (see text). The inset shows a schematic diagram of a sessile droplet that was used in calculating the average height of the droplet (see text).

frames per second using a Fuji Finepix S9600 digital camera. The images were focused on to the camera using an Olympus UPlanFl 10x transmission microscope objective. Examples of snapshots taken from the resulting movies are shown as insets in Figure 2. A movie of the droplet vibrations can also be found online as Supporting Information.

■ RESULTS AND DISCUSSION

An expression for the contact angle dependence of the resonant frequency of sessile droplets can be derived using a method similar to that described by Noblin and co-workers.[12] This simple theory begins by considering standing wave states around the surface of the droplet. Under conditions of resonant vibration the profile length (l) of the droplet (see inset Figure 2) will contain a half integer number of wavelengths (λ), such that,

$$l = 2R\theta = \frac{n\lambda}{2} \tag{1}$$

where R is the radius of curvature of the droplet, θ is the three phase contact angle and n is an integer corresponding to the mode number ($n = 2,3...$).

Droplets that are smaller than the capillary length (~ 2.7 mm for water), can be approximated to the shape of a spherical cap. The volume of a droplet, V, which subtends a contact angle θ with the surface is therefore given by the following:

$$V = \frac{m}{\rho} = \frac{\pi R^3}{3}(\cos^3 \theta - 3\cos \theta + 2) \tag{2}$$

where m is the mass of the droplet and ρ is its density. The dispersion relation for capillary waves on a liquid surface is given by,[20]

$$f = \left(\frac{2\pi\gamma}{\rho\lambda^3}\right)^{1/2} \tag{3}$$

where f is the frequency of vibration and γ is the surface tension of the liquid.

Combining eqs 1, 2, and 3 gives an expression for the contact angle dependence of the frequency of the nth vibrational mode of the droplet;

$$f_n = \frac{\pi}{2}\left(\frac{n^3\gamma}{24m}\frac{(\cos^3\theta - 3\cos\theta + 2)}{\theta^3}\right)^{1/2} \quad (4)$$

This has a similar functional form to the vibration frequencies obtained for free/levitated droplets;[1,13]

$$f_j = \left(\frac{j(j-1)(j+2)\gamma}{3\pi m}\right)^{1/2} \quad (5)$$

where $j = 2,3,4....$ is the mode number. If we approximate $j(j-1)(j+2) \approx j^3$ then a similar functional form to that obtained in eq 4 is recovered to within a geometrical factor which depends upon the contact angle (θ).

According to eq 4, the square of the resonant frequency of the droplet should be inversely proportional to the mass of the droplet. The main panel in Figure 2 shows plots of f^2 vs $1/m$ for droplets supported on the substrates studied here. These plots confirm the functional dependence of the resonant frequency on droplet mass. A consideration of the plots in this figure shows that the contact angle dependence of the slope of f^2 vs $1/m$ is nonmonotonic. Figure 3 shows a plot of the contact angle dependence of this slope along with the predictions of eq 4. The value of γ used to generate the solid line in Figure 3 was 72×10^{-3} Jm^{-2}.[21] The plot of eq 4 shown in Figure 3 displays a clear maximum at a contact angle of $\theta \sim 70°$. This result was also reported by Yamakita and co-workers.[6] The maximum in this plot arises because of the need to fit a half integer number of vibration wavelengths along the profile length of the droplet at resonance. For a fixed mass of droplet and a given mode number, the highest frequency (shortest wavelength) will occur when the profile length, l is a minimum. Inserting R from eq 2 into eq 1 and differentiating gives,

$$\frac{dl}{d\theta} = 2\left(\frac{3m}{\pi\rho}\right)^{1/3}\left(\frac{\cos^3\theta - 3\cos\theta + 2 - \theta\sin^3\theta}{(\cos^3\theta - 3\cos\theta + 2)^{4/3}}\right) \quad (6)$$

The profile length of the droplet is therefore a minimum when $dl/d\theta = 0$. This occurs when the numerator in the second bracket in eq 6 is equal to zero. A plot of this function (not shown) reveals that the minimum in the drop profile length and hence the maximum frequency for a given mass and mode number occurs when $\theta = 70°$ in agreement with Figure 3.

The value of n was chosen to be $n = 2$ for the lowest vibrational frequency of the droplet. Our justification for assigning this mode to the vibrational frequencies shown in Figure 2 comes from the fact that the drop shape expected for the $n = 2$ mode agrees very well with the droplet shapes obtained from the pictures of the vibrating drop shown in the insets in Figure 2. The droplet shown in these images had a mass of 0.0122 ± 0.0001 g and was vibrated at a frequency of 32.6 Hz. This mass and frequency are consistent with the data for droplets on PDMS surfaces shown in Figure 2. We also note that the measured frequencies obtained for droplets on PDMS surfaces agree with the values obtained by Daniel et al.[15] who reported the existence of a sessile drop mode (their so-called "rocking mode") at frequencies that are lower than the lowest vibrational modes associated with levitated drops (the $j = 2$ mode in eq 5). Further

consideration of the drop shapes obtained in the present study reveal that they are also consistent with those predicted by Daniel et al.[15]

At this point it is worth stressing that the frequencies associated with the $n = 2$ mode for sessile droplets are not the same as the $j = 2$ mode of levitated droplets. In the work of Daniel et al.,[15] these authors plotted their frequency data for the "rocking mode" as a function of $1/m$ and compared it to higher vibrational modes of the sessile droplets. The frequency assignments given to the higher modes were based upon the modes associated with levitated droplets. So the $n = 2$ mode discussed by Daniel et al. actually corresponds to the $j = 2$ mode for levitated drops given by eq 5, this is not the same as the $n = 2$ mode for sessile droplets reported here. This point can be illustrated by considering the case when the contact angle is 180° in eq 4— which gives the closest approximation that a sessile drop can achieve to a levitated droplet. In this case, the ratio of frequency of the nth sessile drop mode and the jth levitated drop mode is given by the following:

$$\frac{f_n}{f_j} = \sqrt{\frac{n^3}{8j(j-1)(j+2)}} \quad (7)$$

Inserting $n = j = 2$, we obtain $(f_{n=2})/(f_{j=2}) = (1/8)^{1/2}$, i.e., the lowest frequency mode for the sessile droplet is lower than the lowest frequency mode of the free droplet as observed by Daniel et al. and others.[3] A further consideration of the work of Daniel et al. reveals that the difference between the "rocking mode" and the next highest mode in the vibrational response of sessile droplets (which the authors compare to the levitated drop modes) is consistent with the ratio calculated above. The agreement between the predicted and measured shape of the sessile droplets shown in Figure 2 suggests that the $n = 2$ mode assignment is appropriate for the frequencies measured for the lowest vibrational frequencies of sessile droplets obtained in the present study. Moreover, the fact that this work is consistent with the work of other authors[15] both in terms of the observed drop shapes and the measured frequencies associated with the lowest vibrational modes of sessile drops gives us further confidence in this assignment.

The agreement between the functional form of eq 4 and the measured data is encouraging and suggests that the assumptions made in formulating this model are correct—at least to a first approximation. However, the measured values are consistently smaller than the predictions of this simple model by a factor of 2/3 (see dashed line in Figure 3). This factor probably arises as a result of the simplifying assumptions made in formulating the model. The first assumption relates to the use of the spherical cap approximation used in eq 2. This approximation assumes that the dominant contribution in determining the shape of the droplets arises due to surface tension and neglects the effects of gravity. A simple calculation using eq 2 shows that for contact angles $\theta > 30°$, the radius of curvature of the drops, $R = (3m/\pi\rho(\cos^3\theta - 3\cos\theta + 2))^{1/3}$, is typically less than the capillary length of water $L_{cap} = ((\gamma)/(\rho g))^{1/2} \sim 2.7$ mm (assuming acceleration due to gravity $g = 9.8$ ms^{-1}, $\gamma = 72$ mJm^{-2} and $\rho = 1000$ kgm^{-3}). In this regime, the spherical cap approximation is an acceptable one for the droplet shape over the range of droplet masses studied. However for contact angles less than 30°, the radius of curvature begins to exceed the capillary length of water and the effects of gravity start to become important in determining the droplet shape. These simple calculations are confirmed by

similar, but more detailed calculations based on the studies by Rodriguez-Valverde and co-workers,[22] which indicate that capillary effects dominate when the droplet volume $V \leq 0.1 L_{cap}{}^3$. Another potential source of error in the model relates to the fact that the expression used to describe the dispersion properties of the liquid surface in eq 3 is only valid for an infinitely deep bath of liquid[20] and is unlikely to be directly applicable to small liquid droplets in an unmodified form. In fact, this expression is only expected to be valid when the distance from the surface of the droplet to the substrate is much larger than the characteristic length scale associated with the vibrations $\sim\lambda/2\pi$. From simple geometry, the height of a point on the surface of a spherical cap which has a radius of curvature, R, is given by $h = R(\cos \phi - \cos \theta)$, where ϕ is the angle subtended at the center of curvature between the point and the vertical axis of the drop (see inset in Figure 3). The average height,$\langle h \rangle$, of the droplet is then given by the following:

$$\langle h \rangle = \frac{R}{2\theta} \int_{-\theta}^{\theta} (\cos \phi - \cos \theta) d\phi = R\left(\frac{\sin \theta}{\theta} - \cos \theta\right) \quad (8)$$

If $\lambda/2\pi \ll \langle h \rangle$, then inserting λ from eq 1 we have the condition that eq 3 is satisfied when $(2\theta)/(n\pi) + \cos \theta - (\sin \theta)/(\theta) \ll 0$. This inequality is only valid for large values of n and for contact angles larger than $\sim 110°$, indicating that the expressions in eq 3 and eq 4 are not strictly valid for $n = 2$ and for small contact angles.

Another factor which is neglected in the model relates to the effects of damping on the droplets[1,10] due to viscous dissipation within the drop. The influence of damping has not been incorporated into the model. However, if the vibrating drops are considered to be damped harmonic oscillators, then the inclusion of damping in the system would be expected to reduce the measured resonant frequencies relative to those predicted by eq 4. We note that these damping effects are likely to be contact angle dependent and that the results shown in Figure 3 indicate that a constant scaling factor of ~ 0.81 exists between the measured resonant frequencies of the sessile droplets and those predicted by equation eq 4 over the entire range of contact angles. This does not seem to be consistent with the idea that viscous damping effects in the droplets alone are responsible for shifting the resonant frequency of the lowest frequency mode of the droplets relative to the calculated values. The contact angle dependence of dissipation effects in the sessile droplets will form the subject of future studies.

Despite all of the limitations of the model discussed above, the level of agreement between the dashed line corresponding to the modified version of the model and the data are very good. Any small remaining differences are attributed to variations in the surface tension of the water droplets used in this work that occur as the result of the presence of small impurities and/or errors in the measured contact angles obtained using the simple webcam based approach.

CONCLUSIONS

A simple method for the optical detection of droplet vibrations was used to measure the contact angle dependence of the lowest frequency vibrational modes of sessile water droplets. The measured frequencies were found to be consistent with a previously observed low frequency "rocking mode" in sessile drops. They were also found to be in agreement (to within a factor of 0.81) with the predictions of a simple theory which considers the frequencies associated with standing wave states along the profile length of the droplets.

ASSOCIATED CONTENT

ⓢ Supporting Information.   A short movie entitled dropwobble.avi has been uploaded as Supporting Information. This movie shows the vibration of a 0.0122 g water droplet vibrated on a PDMS surface at a frequency of 32.6 Hz. The movie was collected at a frame rate of 60 fps, but has been reduced to make the droplet oscillations easier to see. There is also some aliasing of the droplet motion due to the vibration frequency and the frame rate used to acquire the images. This material is available free of charge via the Internet at http://pubs.acs.org.

AUTHOR INFORMATION

Corresponding Author
*E-mail: james.sharp@nottingham.ac.uk.

ACKNOWLEDGMENT

REFERENCES

(1) Chandrasekhar, S. *Proc. London Math. Soc.* **1959**, *3* (9), 141–149.

(2) Wilkes, E. D.; Basaran, O. A. *Phys. Fluids* **1997**, *9* (6), 1512–1528.

(3) Strani, M.; Sabetta, F. *J. Fluid Mech.* **1984**, *141*, 233–247.

(4) Smithwick, R. W., III; Boulet, J. A. M. *J. Colloid Interface Sci.* **1989**, *130*, 588–596.

(5) Hill, R. J. A.; Eaves, L. *Phys. Rev. E* **2010**, *81*, 056312.

(6) Yamamkita, S.; Matsui, Y.; Shiokawa, S. *Jpn. J. Appl. Phys.* **1999**, *38*, 3127–3130.

(7) Daniel, S.; Sircar, S.; Gliem, J.; Chaudhury, M. K. *Langmuir* **2004**, *20*, 4085–4092.

(8) Langley, K. R.; Sharp, J. S. *Langmuir* **2010**, *26* (23), 18349–18356.

(9) Shastry, A.; Case, M. J.; Bohringer, K. F. *Langmuir* **2006**, *22*, 6161–6167.

(10) Ghosh, S.; Sharma, P.; Bhattacharya, S. *Rev. Sci. Instrum.* **2007**, *78*, 115110.

(11) Celestini, F.; Kofman, R. *Phys. Rev. E* **2006**, *73*, 041602.

(12) Noblin, X.; Buguin, A.; Brochard-Wyart, F. *Eur. Phys. J. Special Topics* **2009**, *166*, 7–10.

(13) McHale, G.; Elliot, S. J.; Newton, M. I.; Herbertson, D. L.; Esmer, K. *Langmuir* **2009**, *25*, 529–533.

(14) Oh, J. M.; Ko, S. H.; Kang, K. H. *Langmuir* **2008**, *24*, 8379–8386.

(15) Daniel, S.; Chaudhury, M. K.; DeGennes, P. G. *Langmuir* **2005**, *21*, 4240–4248.

(16) Noblin, X.; Buguin, A.; Brochard-Wyart, F. *Eur. Phys. J. E* **2004**, *14*, 395–404.

(17) Karadag, Y.; Jonas, A.; Tasaltin, N.; Kiraz, A. *Appl. Phys. Lett.* **2011**, *98*, 194101.

(18) Mugele, F.; Baret, J. C.; Steinhauser, D. *Appl. Phys. Lett.* **2006**, *88*, 204106.

(19) Rodriguez-Valverde, M. A.; Montes Ruiz-Cabello, F. J.; Cabrerizo-Vilchez, M. A. *Soft Matter* **2011**, *7*, 53.

(20) Landau, L. D. Lifshitz, E. M. *Fluid Mechanics*, 2nd ed.; Elsevier: Oxford, 1987; p 245.

(21) Israelachvili, J. *Intermolecular and Surface Forces*, 2nd ed.; Elsevier: London, 1991; p 351

(22) Rodriguez-Valverde, M. A.; Montes Ruiz-Cabello, F. J.; Cabrerizo-Vilchez, M. A. *Adv. Colloid Interface Sci.* **2008**, *138*, 84–100.